Inorganic Chemistry Communications 153 (2023) 110845

Contents lists available at ScienceDirect

Inorganic Chemistry Communications

journal homepage: www.elsevier.com/locate/inoche

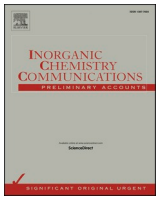

Short communication

Green synthesis of carbon quantum dots from *Sideritis vuralii* and its application in supercapacitors

Canan Başlak [a], Gülşah Öztürk [b], Serkan Demirel [c], Adem Kocyigit [d,*], Süleyman Doğu [e], Murat Yıldırım [b]

[a] Department of Chemistry, Science Faculty, Selcuk University, Konya, Turkey
[b] Department of Biotechnology, Science Faculty, Selcuk University, Konya, Turkey
[c] Department of Electric and Energy, Vocational High School, Igdir University, Igdir, Turkey
[d] Department of Electronics and Automation, Vocational High School, Bilecik Seyh Edebali University, Bilecik, Turkey
[e] Department of Medical and Aromatic Plants, Meram Vocational School, Necmettin Erbakan University, Konya, Turkey

ARTICLE INFO

Keywords:
CQDs
Green synthesis
S. vuralii
Supercapacitors

ABSTRACT

Quantum dots have good optical and electrical behaviors and can be employed in solar cells, displays and supercapacitors. When new studies in nanoparticle as well as synthesis of quantum dots are examined, it can be seen that the interest in the green synthesis approach has increased. The green synthesis approach is so prominent due to an environmentally friendly method and does not contain toxic chemicals at the experimental stage. In this study, we used *Sideritis vuralii (S. vuralii)*, which is endemic in Turkey, as a source of the green synthesis approach. We synthesized carbon quantum dot (CQDs) particles with the hydrothermal method from *S. vuralii* plant. We performed UV–Vis spectra, fluorescence spectra, XPS and DLS analyzes for the characterization of the CQDs. According to the size and characteristics results, the CQDs were successfully synthesized from the *S. vuralii* plant. Furthermore, we employed CQDs as electrode for capacitor applications, and cyclic voltammetry (CV) measurements were performed. The CV measurements indicated that CQDs electrodes have rechargeable symmetrical capacitor behaviors with 10.42 F/g charge, 8.26 F/g discharge capacitances. The green synthesized CQDs can be improved for supercapacitor applications.

1. Introduction

Due to the small size of the nanoparticles (1–100 nm) and their large surface areas, the desired changes in the material can be achieved more easily to use them in various applications [1,2]. There are two generally accepted approaches when considering the production of nanomaterials. The top-down strategy includes reducing the structure to the nanoscale. In contrast, the bottom-up strategy involves building larger nanostructures from smaller atoms and molecules [3,4]. One way of nanoparticle production is hydrothermal synthesis. Hydrothermal synthesis is based on the production of quality crystal particles in nano and micro sizes from solution at high vapor pressure and high temperature [5]. The essence of the technique is to synthesize suitable reagents, in aqueous or non-aqueous solutions, at certain temperature values in special containers called autoclaves, which consist of Teflon-coated outer steel [6].

Quantum dots, whose typical sizes range from nanometers to several microns, and whose size, shape and interactions can be precisely controlled using advanced nanofabrication technology, have tunable bandwidth because they have size variations [7,8]. Quantum dots (QDs) are usually semiconductor nanocrystals with physical dimensions smaller than the exciton Bohr radius, and carbon quantum dots (CQDs, C-dots or CDs), which are generally small carbon nanoparticles (less than 10 nm) with various unique properties, have been found wide use in more and more fields over the past few years [9,10]. Many people refer to quantum dots as “artificial atoms”. A series of quantum dots can form an artificial two-dimensional crystal. In conclusion, this shows that it is possible to create new artificially engineered quantum dot materials [11]. The exceptional optical and fluorescence properties of carbon quantum dots enable them to be used in a variety of cutting-edge applications [12].

Using a green method in chemical synthesis is advantageous because there are no hazards associated with the use of harmful solvents [13,14]. Green synthesis has superior properties, and is non-toxic, environmentally friendly, and low-cost method. CQDs can be synthesized using various sources such as plants [15,16], fungi [17] and many living materials found in nature. It is possible to make green synthesis with

* Corresponding author at: Vocational High School, Department of Electronic and Automation, Bilecik Seyh Edebali University, Bilecik, Turkey.

https://doi.org/10.1016/j.inoche.2023.110845
Received 12 March 2023; Received in revised form 11 May 2023; Accepted 16 May 2023
Available online 19 May 2023

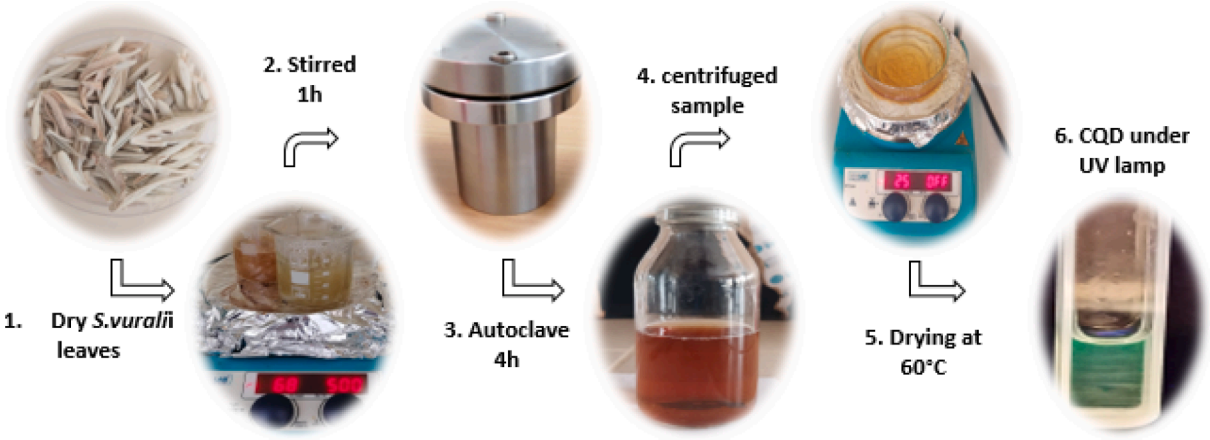

Fig. 1. CQDs synthesis diagram.

many things found in nature that are harmless to health. To summarize briefly, it is known that green synthesis can be thought a biological method in which nanoparticles are easily obtained [1].

Supercapacitors, also known as ultracapacitors, power capacitors, electrochemical capacitors or electrochemical double layer capacitors, are ideal power storage systems with advantages such as much greater energy density, short charging times and long life compared to conventional capacitors [18]. A capacitor is a circuit element that is used to store an electric charge for a short time, by dividing the polarity of the electrons and storing them in the electric field. It is formed by placing an insulating material between two metal electrodes [19]. The working systems of capacitors and supercapacitors are similar. However, energy storage systems are different from each other. While the energy charges in the capacitor accumulate on the plate, they are accumulated on the

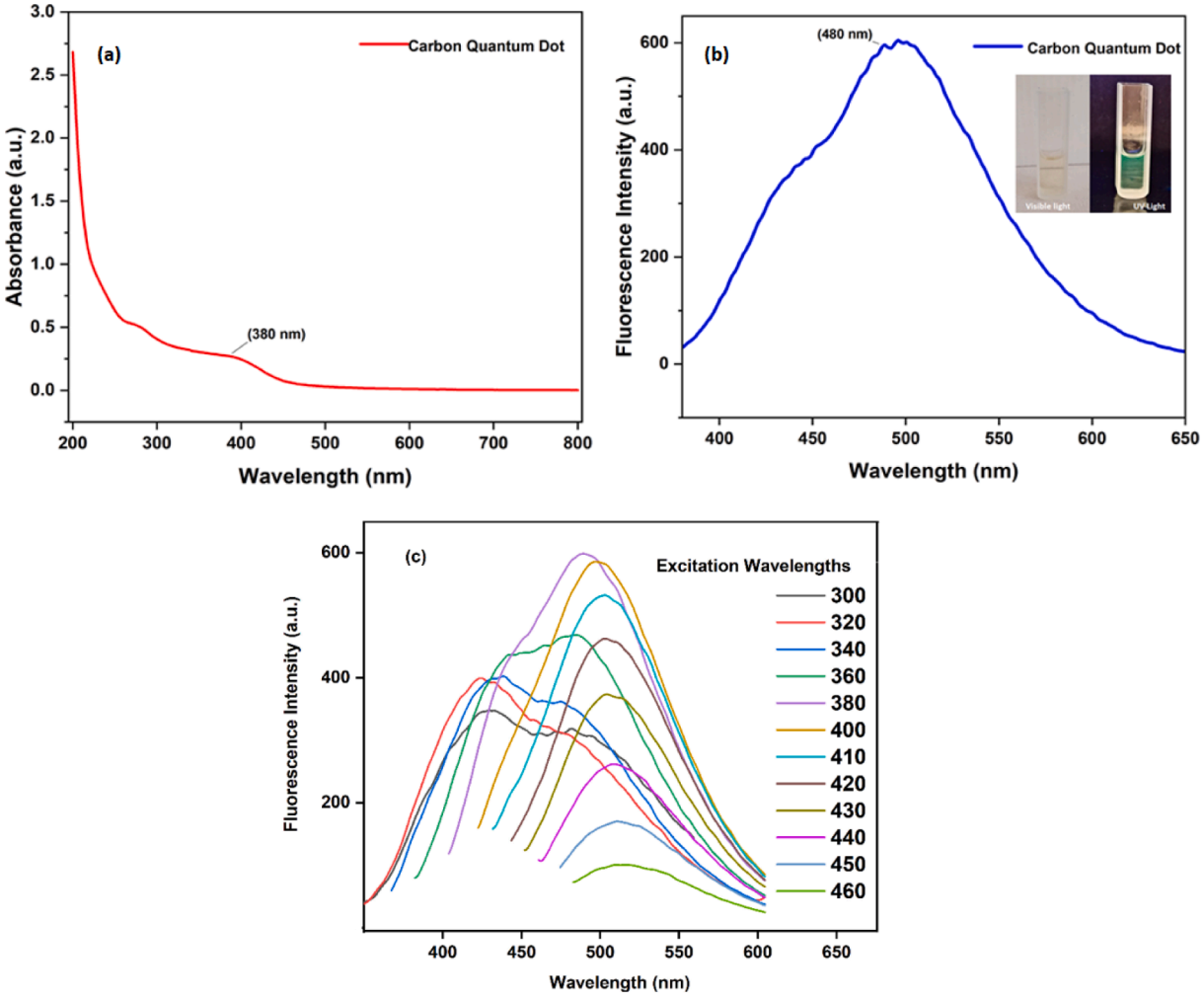

Fig. 2. a) UV–vis absorbance spectra, **b)** fluorescence emission spectra of CQDs by excitation at 380 nm, and **c)** fluorescence emission spectra of CQDs for various excitation wavelengths.

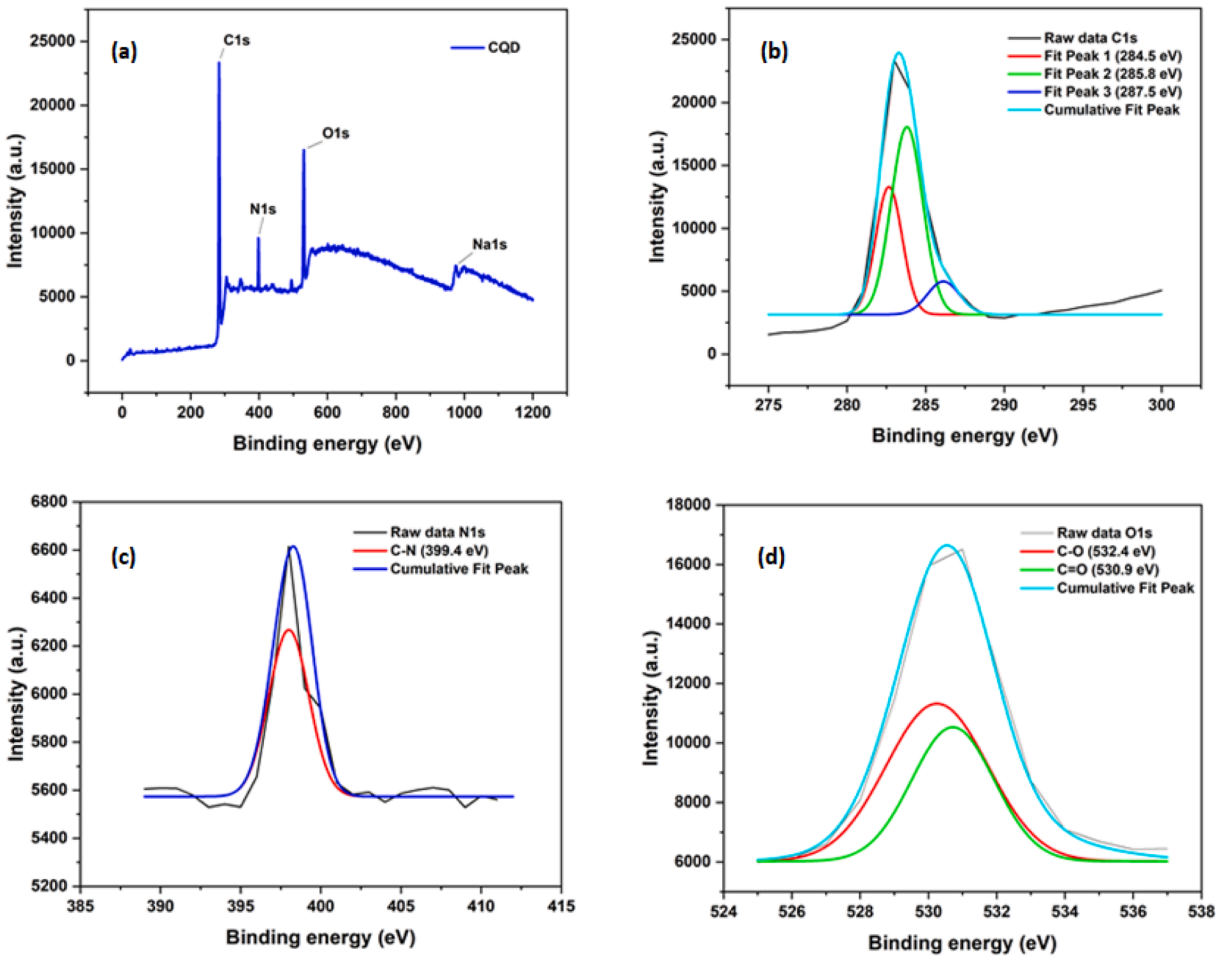

Fig. 3. a) XPS survey spectrum, **b)** C1s, **c)** N1s, and **d)** O1s for CQDs.

electrode and electrolyte separator with the storage system of these energy loads in the supercapacitors, and thus supercapacitors reach high capacitance values [20].

In this study, we obtained CQDs by hydrothermal method with the green synthesis of the leaves of *Sideritis,* a plant genus from the *Lamiaceae* family. To the best of our knowledge, *Sideritis* has never been used as CQDs source due to its rareness and endemically distribution. *Sideritis* (Labiatae) is represented in Turkey by 52 taxa belonging to 44 species, 34 of which are endemic to Turkey [21]. Sideritis species are widely used as herbal tea and folk medicine in Turkey [22]. The synthesized quantum dots were employed for supercapacitor electrodes and tested by CV measurements in a Swagellok-type cell.

2. Experimental

2.1. CQDs synthesis by hydrothermal method from Sideritis vuralii leaves

Dry *Sideritis vuralii* leaves were grinded with a grinder. 0.5 g ground leaves were taken into 60 ml pure water and mixed in magnetic stirrer at 400 rpm and 60 °C for 1 h to obtain homogeneous solution. 1 ml ethylenediamine (EDA) was added into the homogeneous solution. The solution was placed into the Teflon-lined stainless steel autoclave. An oven was set 140 °C for 4 h, and autoclave was put into the oven reaching 140° C. After 24 h, the autoclave taken from the oven was opened. The sample was centrifuged at 4000 rpm for 3 min. Ultracentrifuge was applied to the separated liquid sample at 15000 rpm for 10 min to remove large particles. To obtain purer and finer particles, sample was passed through a syringe filter. The purified sample was dried in a glass petri dish at room temperature for 48 h. The whole synthesis steps as a diagram are shown in Fig. 1.

2.2. Electrochemical studies

The Swagellok-type cell was used for capacitor formation. To measure the electrode properties, 2 pieces same shaped stainless-steel foils with a diameter of 1 cm were used as electrode substrates. Afterward, equal amount (0.01 g) of CQDs was dropped onto these substrates. The stainless-steel substrates were used as current collector of electrodes because of having high electrical conductivity and high chemical surface resistance, and to prevent the electrodes from redox reactions between sample-current collectors. 6 M $KOH_{(aq)}$ solution and cellulosic paper membrane was used as electrolyte and membrane, respectively. The cyclic voltammetry (CV) measurements were carried out for constant scan speeds of 200, 400, 800 and 1200 mV/s. The CV measurements were conducted as 3 cycles to observe any anomalies, but only one CV cycle data was given in the result section to avoid data analyses confusion. In order to measure the capacitance, the two-electrode method was exploited. The cycle life study capacitance measurements were performed under 200 mV/s constant scanning speed in the range of 0–2 V for 1000 cycles. Then, capacitance values of the samples are calculated as in ref [17]. The capacity retention values were calculated as in ref [23], and, the energy and power density values has been calculated as in ref [24].

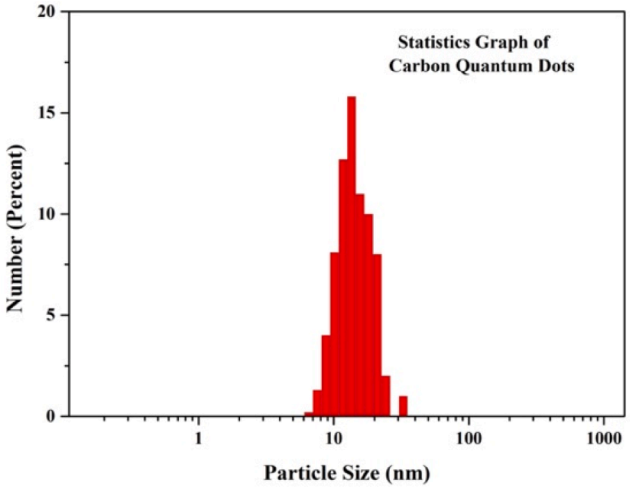

Fig. 4. Particle size distribution histogram of CQDs.

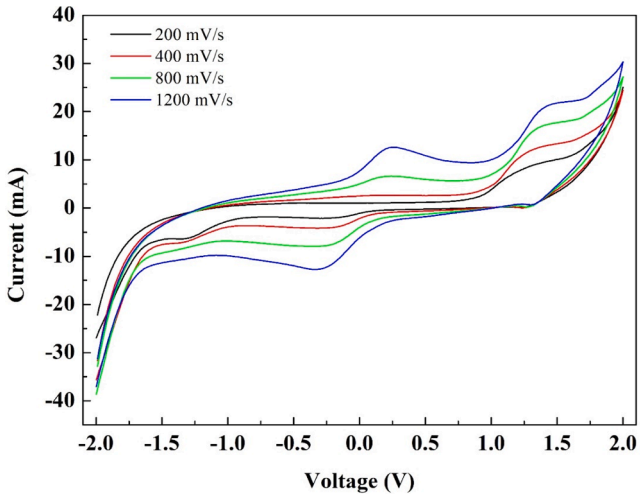

Fig. 5. Some redox reactions and electrolyte polarization effect on CV.

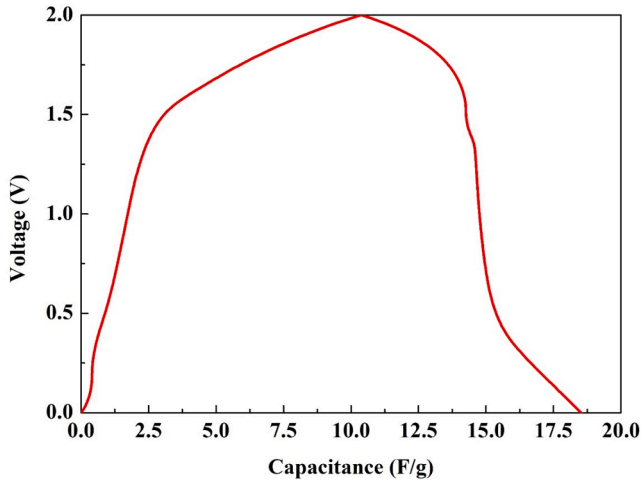

Fig. 6. CQDs first cycle capacitive performance.

2.3. Instruments and characterization

The spectrometric properties of CQDs were measured on a LS 55 fluorescence spectrophotometer. The ultraviolet–visible (UV–Vis) absorption spectrum was measured in a UV-1280 (Shimadzu) spectrophotometer. To determine surface chemistry of the nanomaterials, X-ray photoelectron spectroscopy (XPS) analysis was performed with a monochromatic Al/K_α (Thermo-K-Alpha) as the X-ray source. For qualitative and quantitative examinations of CQDs, X-ray Diffractometer (XRD) analysis was performed with Bruker Advance D8 brand X-ray Diffractometer. Dynamic light scattering (DLS) analysis was performed with a MALVERN/ DLS MPT2 instrument to measure the intensity and variation of light scattered from small particles in dilute solution of CQDs. The electrochemical performance analyses were conducted with Gamry 1010-E Potentiostat.

3. Results and discussion

UV–Vis spectroscopy analyses were performed to measure absorption wavelength of the synthesized nanoparticles. Fig. 2a and 2b show absorption and fluorescence spectra of the CQDs, respectively. Synthesized CQDs exhibited two peaks at around 260 and 380 nm as shown in Fig. 2a. These absorption peaks at 260 nm and 330 nm are attributed to π-π* transition of carbon and n-π* transition of C = O, respectively. The fluorescence emission of these CQDs is a maximum in the range of 480 nm according to Fig. 2b. The CQDs exhibited green radiation under the UV lamp. These results revealed that the CQDs are of the desired particle size for supercapacitor applications. Fluorescence measurements were repeated for different excitation wavelengths. Fig. 2c shows fluorescence measurements of the CQDs for various excitation wavelengths. A double peak seen before 380 nm and 380 nm was chosen as the working excitation wavelength since the most intense emission was at 380 nm. This situation is in accordance with the literature, and it is seen that it can be encountered when natural foods or plant species are used for carbon dot synthesis. As a possible feature of CQDs, by changing the excitation peaks, it is seen that the emission peaks shift to the right, and the peak ridge on the left disappears [25].

XPS analysis was performed to obtain chemical information about the surface of the synthesized CQDs. Fig. 3 displays XPS analysis of the synthesized CQDs. According to the results, 284.5 eV, 399.4 eV and 532.4 eV can be attributed to C = C, C-N, and C-O interactions, respectively [26-29]. As shown in the Fig. 3a, there is pollution in transport water that occur 1050 eV. The peak of Na1s [30,31] at 1050 eV is thought to be due to contamination in the transport water.

DLS analysis was performed to determine the particle size distribution of synthesized CQDs. The DLS measurement of the solution prepared with a suitable dilution was taken by mixing the medium thoroughly. According to the results of the analysis, the particle size distribution of CQDs is well below 20 nm (Fig. 4).

3.1. Electrochemical performance analyses

The CV analyzes were performed firstly for electrochemical analyze studies. Fig. 5 shows redox reactions and electrolyte polarization effect of the CQDs. The CV measurements were performed in the range of ± 2 V, and a single anodic reaction was observed between 0 and 2 V up to 400 mV/s scanning speed while second anodic reaction was observed at 800 and 1200 mV/s scanning rates. Moreover, only a single redox reaction is observed in the cathodic zone, turning from 2 V to 0. This situation may be caused by electrode–electrolyte interactions. The second redox reaction occurring between 0 and 0.5 V after 400 mV/s scanning speed may result from the oxidation of K^+ ions during the anodic polarization of the electrolyte. In this reaction that may occur on the electrode surface, it appears as anodic redox because the K^+ ion cannot be completely separated from the surface.

The measurements were continued up to the level of −2 V. The continuation of the capacitive current plateaus especially in the (-2)-0 V region and the similar situation in the (-1)-0 V range as in 2–0 V range, supports the electrolyte origin of the second redox reaction. This shows

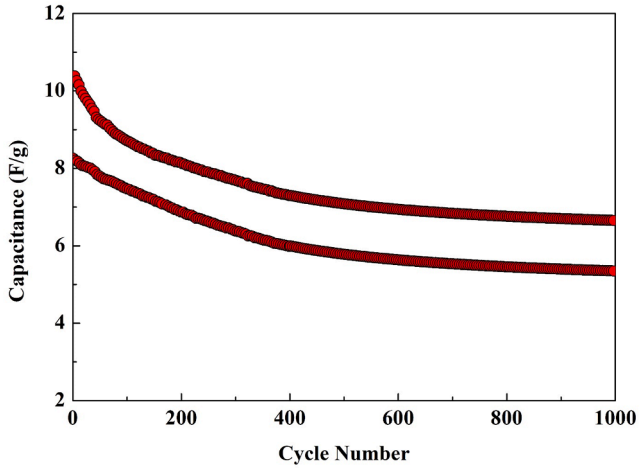

Fig. 7. Cycle life performance of symmetric CQDs capacitors.

that the $KOH_{(aq)}$ electrolyte cannot operate at high speeds with full efficiency. On the other hand, the CV patterns at all scan rates showed a permanent capacitive hysteresis feature, and capacitor formation was achieved with CQDs electrodes. Furthermore, characteristic redox reactions were determined that occurring between 1 and 2 V (for both anodic and cathodic sites) in Fig. 5. According to literature, it is thought that these reactions are caused by electrolyte-derived Faradaic C = O or C-OH bonds [32]. These reactions are also observed in the anodic and cathodic regions also indicate that the electrodes have rechargeable properties.

After the permanent capacitive current plateaus seen in the CV analyzes, the charge and discharge analyze were performed for capacitor analysis. In Fig. 6, the first charge–discharge performance of CQDs symmetric capacitors has been indicated. The CQDs symmetrical capacitors have been determined to have 10.42 F/g charge, 8.26 F/g discharge capacitance. Similar to CV analyze, the effects of redox reactions seen in CV analysis were detected again in the first charge–discharge patterns. According to these values, the *Sideritis vanalii* CQDs can be thought as supercapacitor electrode active materials. Although the supercapacitor electrode performance exhibits, it has been observed that there is a difference between the charge and discharge capacities. This situation may be related to CV scan speeds between 200 and 1200 mV/s can be considered high-speed charge–discharge, and it is thought that such capacity losses in *Sideritis vanalii* CQDs electrodes are based on electrode polarization performance for high-speed scanning. In other words, insufficient ion diffusion rate in high-speed charge–discharge process affects the electrode polarization, results in a decrease in the redox effect of the electrodes, and therefore causes the differences between the charge discharge capacitances.

After the first charge–discharge capacitance analysis, 1000 cycles of capacitive performance analysis were performed. Fig. 7 exhibits cycle life performance of symmetric CQDs capacitors. The charge and discharge capacitance values decreased to 6.67 F/g and 5.34 F/g, respectively at the end of 1000 cycles for the scanning speed of 200 mV/s. It is known that under normal conditions, the carbon-based electrodes provide high performance for supercapacitors [33]. The "High Performance" means that the coulombic efficiency between charge–discharge capacitances is 95% and above. It is also known that capacity retention percentages are very low in these capacitors [34].

Table 1 tabulates the capacitive performances of the CQDs electrodes for the 1st, 50^{th}, 100^{th}, 250^{th}, 500^{th}, 750^{th} and 1000^{th} cycles. The CQDs symmetric capacitors have an average of 82% coulombic efficiency performance during 1000 cycles. In addition, a capacity loss of 35% was experienced after 1000 cycles. Despite the high-capacity loss, structural stability was determined after an average of 400 cycles. The capacity loss decreased after 400 cycles and remained at the average level of 5%. The Energy and Power density values were also calculated within the scope of the study. As a result of the calculations, the energy storage amount at the level of 4.59 mW/g decreased to the level of 2.97 mW/g at the end of 1000 cycles, and the power density decreased from 3.30 Wh/g to 2.14 Wh/g.

Table 2 shows the comparison of symmetric capacitor capacitance performances formed with *Sideritis vanalii* CQDs electrodes with Milk-CQDs (carbon-quantum-dots from waste milk), CQDs-PPy (carbon-quantum-dots from nanocomposite using polypyrrole), CDs/Graphene (carbon-dots with graphene) electrodes. According to the capacitance values in this comparison, the *Sideritis Viralii* CQDs supercapacitors have a higher capacitance value than CQDs-PPy capacitors and slightly lower than others. However, as can be seen from the Milk-CQDs capacitance values, the charge–discharge capacitance values may vary according to the applied current and voltage values. In particular, the capacitance of 24.15 F/g obtained from CDs/Graphene capacitors was obtained at a scanning rate of 100 mV/s. On the other hand, the discharge capacitance of 8.26 F/g was obtained at 200 mV/s in *Sideritis Viralii* CQDs supercapacitor. Considering that, higher capacitance values can be obtained at lower scanning rates. According to these results, *Sideritis Viralii* CQDs supercapacitors can be thought a suitable electrode active material in terms of technological applications with high capacitive performance.

4. Conclusion

We synthesized CQDs by hydrothermal method and characterized by UV–Vis spectroscopy, fluorescence spectroscopy, XPS and DSL analyses. The synthesized CQDs were tested for supercapacitor applications in a Swagellok-type cell by CV measurements. While the absorption spectra

Table 2
Comparison of CQDs capacitor performances.

Electrode	Potential Window	Capacitance	Reference
Milk-CQD	0–0.8 V	95 F/g (at 0.12 A/g) 40 F/g (at 0.2 A/g)	[35]
CQD-PPy	(-0.2)-1 V	0.24 F/g (at 150 mV/s)	[36]
CDs/Graphene	0–3 V	24.15F/g (at 100 mV/s)	[37]
KF-CQDs	0–1 V	15.13F/g (200 mV/s)	[17]
Sideritis vuralii CQDs	0–2 V	8.26 F/g (200 mV/s)	This Study

Table 1
Performance values of *Sideritis vanalii* CQDs symmetric capacitors in some specific cycles.

Cycle No	Charge Capacitance (F/g)	Discharge Capacitance (F/g)	Colombic Efficiency (%)	Discharge Capacity Retention (%)	Energy Density (mW/g)	Power Density (Wh/g)
1	10.42	8.26	79	–	4.59	3.30
50	9.24	7.79	84	5.69	4.33	3.12
100	8.71	7.46	85	9.68	4.14	2.98
250	7.89	6.62	84	19.85	3.68	2.65
500	7.08	5.78	82	30.02	3.21	2.31
750	6.79	5.49	81	33.53	3.05	2.2
1000	6.65	5.34	80	35,35	2.97	2.14

revealed peak at 380 nm, fluorescence spectra exhibited peak at around 480 nm as green radiation for CQDs. XPS analysis deduced C = C, C-N, and C-O interactions related to 284.5 eV, 399.4 eV and 532.4 eV, respectively. The particles size of CQDs changed between the 10 nm and 20 nm according to DSL measurements. The CV measurements indicated that CQDs electrodes have rechargeable properties symmetrical capacitor behaviors with 10.42 F/g charge, 8.26 F/g discharge capacitances. The green synthesized CQDs can be improved for supercapacitor applications.

Declarations.

Funding.

There is no funding for this research.

Data availability.

Data are available upon reasonable request.

Conflict of interests.

There is no any conflict of interest.

CRediT authorship contribution statement

Canan Başlak: Investigation, Methodology. **Gülşah Öztürk:** Methodology, Data curation. **Serkan Demirel:** Investigation, Methodology, Data curation, Writing – original draft. **Adem Kocyigit:** Writing – review & editing. **Süleyman Doğu:** Investigation, Methodology. **Murat Yıldırım:** Writing – review & editing.

Declaration of Competing Interest

The authors declare that they have no known competing financial interests or personal relationships that could have appeared to influence the work reported in this paper.

Data availability

Data will be made available on request.

References

[1] A. Eren, M.F. Baran, Fıstık (Pistacia vera L.) yaprağından gümüş nanopartikül (agnp)'lerin sentezi, karakterizasyonu Ve antimikrobiyal aktivitesinin incelenmesi, Türkiye Tarımsal Araştırmalar Derg. 6 (2) (2019) 165–173, https://doi.org/10.19159/tutad.493006.

[2] S. Sundar, J. Kundu, S.C. Kundu, Biopolymeric nanoparticles, Sci. Technol. Adv. Mater. 11 (1) (Feb. 2010) 014104, https://doi.org/10.1088/1468-6996/11/1/014104.

[3] N. Abid, et al., Synthesis of nanomaterials using various top-down and bottom-up approaches, influencing factors, advantages, and disadvantages: A review, Adv. Colloid Interface Sci. 300 (Feb. 2022) 102597, https://doi.org/10.1016/j.cis.2021.102597.

[4] P. Christian, F. Von der Kammer, M. Baalousha, T. Hofmann, Nanoparticles: structure, properties, preparation and behaviour in environmental media, Ecotoxicology 17 (5) (Jul. 2008) 326–343, https://doi.org/10.1007/s10646-008-0213-1.

[5] P. Wu, W. Li, Q. Wu, Y. Liu, S. Liu, Hydrothermal synthesis of nitrogen-doped carbon quantum dots from microcrystalline cellulose for the detection of Fe3+ ions in an acidic environment, RSC Adv. 7 (70) (Sep. 2017) 44144–44153, https://doi.org/10.1039/C7RA08400E.

[6] T.A. Dontsova, S.V. Nahirniak, I.M. Astrelin, Metaloxide nanomaterials and nanocomposites of ecological purpose, J. Nanomater. 2019 (Apr. 2019) 1–31, https://doi.org/10.1155/2019/5942194.

[7] C. Öksel, Y. Koç, H. Yağli, A. Koç, Kuantum Noktalı Güneş Hücreleri, Nevşehir Bilim ve Teknol. Derg. vol. 7, no. 20(18) (2018) 174–182, https://doi.org/10.17100/nevbiltek.372448.

[8] L. Kouwenhoven, C. Marcus, Quantum dots, Phys. World 11 (6) (1998) 35–40, https://doi.org/10.1088/2058-7058/11/6/26.

[9] Y. Wang, A. Hu, Carbon quantum dots: Synthesis, properties and applications, J. Mater. Chem. C 2 (34) (2014) 6921–6939, https://doi.org/10.1039/c4tc00988f.

[10] P.G. Luo, et al., Carbon 'quantum' dots for optical bioimaging, J. Mater. Chem. B 1 (16) (2013) 2116–2127, https://doi.org/10.1039/c3tb00018d.

[11] E. Borovitskaya and M. S. Shur, *Quantum Dots*, Second., vol. 25. Danver, USA: WORLD SCIENTIFIC, 2002. doi: 10.1142/4934.

[12] J. Prasad, C. Shobana, M. Ragupathi, R. Kalai, A sustainable green synthesis of functionalized biocompatible carbon quantum dots from Aloe barbadensis miller and its multifunctional applications, Environ. Res. vol. 200, no. May (2021) 111414, https://doi.org/10.1016/j.envres.2021.111414.

[13] A. Alharbi, et al., Green synthesis approach for new Schiff ' s-base complexes; theoretical and spectral based characterization with in-vitro and in-silico screening, J. Mol. Liq. 345 (2022) 117803, https://doi.org/10.1016/j.molliq.2021.117803.

[14] S. Demirel, M.S. Nas, A. Kocyigit, M.H. Calimli, M.H. Alma, Astragalus brachycalyx fischer roots-derived porous carbon integrated with a novel NiSnO2/PC nanocomposite for high-performance supercapacitors, J. Mater. Sci. Mater. Electron. 34 (5) (Feb. 2023) 1–13, https://doi.org/10.1007/s10854-023-09894-7.

[15] G. Chellasamy, S.K. Arumugasamy, S. Govindaraju, K. Yun, Green synthesized carbon quantum dots from maple tree leaves for biosensing of Cesium and electrocatalytic oxidation of glycerol, Chemosphere 287 (P1) (2022) 131915, https://doi.org/10.1016/j.chemosphere.2021.131915.

[16] G. Ge, et al., Green synthesis of nitrogen-doped carbon dots from fresh tea leaves for selective Fe3+ ions detection and cellular imaging, Nanomaterials 12 (6) (2022) pp, https://doi.org/10.3390/nano12060986.

[17] C. Baslak, S. Demirel, A. Kocyigit, H. Alatli, M. Yildirim, Materials Science in Semiconductor Processing Supercapacitor behaviors of carbon quantum dots by green synthesis method from tea fermented with kombucha, Mater. Sci. Semicond. Process. vol. 147, no. April (2022) 106738, https://doi.org/10.1016/j.mssp.2022.106738.

[18] Z. Xu, J. Zhao, H. Li, K. Li, Z. Cao, J. Lu, Influence of the electronic configuration of the central metal ions on catalytic activity of metal phthalocyanines to Li/SOCl2 battery, J. Power Sources 194 (2) (Dec. 2009) 1081–1084, https://doi.org/10.1016/j.jpowsour.2009.06.047.

[19] J. Sun, B. Luo, H. Li, A review on the conventional capacitors, supercapacitors, and emerging hybrid Ion capacitors: Past, present, and future, Adv. Energy Sustain. Res. 3 (6) (Jun. 2022) 2100191, https://doi.org/10.1002/aesr.202100191.

[20] Subasinghage, Gunawardane, Padmawansa, Kularatna, Moradian, "Modern supercapacitors technologies and their applicability in mature electrical engineering applications," energies, Multidisciplinary Digital Publishing Institute. 15 (20) (2022) 7752, https://doi.org/10.3390/en15207752.

[21] K.H.C. Baser, Aromatic biodiversity among the flowering plant taxa of Turkey, Pure Appl. Chem. 74 (4) (Jan. 2002) 527–545, https://doi.org/10.1351/pac200274040527.

[22] N. Kirimer, N. Tabanca, G. Tümen, H. Duman, K.H.C. Başer, Composition of the essential oils of four endemic Sideritis species from Turkey, Flavour Fragr. J. 14 (6) (1999) 421–425, https://doi.org/10.1002/(SICI)1099-1026(199911/12)14:6<421::AID-FFJ852>3.0.CO;2-Z.

[23] K. Cicek, S. Demirel, Self-healable PVA–graphite–borax as electrode and electrolyte properties for smart and flexible supercapacitor applications, J. Mater. Sci. Mater. Electron. 32 (12) (Jun. 2021) 16335–16345, https://doi.org/10.1007/s10854-021-06186-w.

[24] D. Hu, et al., Optimization the energy density and efficiency of BaTiO3-based ceramics for capacitor applications, Chem. Eng. J. 409 (Apr. 2021) 127375, https://doi.org/10.1016/j.cej.2020.127375.

[25] T. Pal, S. Mohiyuddin, G. Packirisamy, Facile and green synthesis of multicolor fluorescence Carbon dots from curcumin. In vitro and in vivo bioimaging and other applications, ACS Omega 3 (1) (Jan. 2018) 831–843, https://doi.org/10.1021/acsomega.7b01323.

[26] S. Sarkar, et al., Graphene quantum dots from graphite by liquid exfoliation showing excitation-independent emission, fluorescence upconversion and delayed fluorescence, Phys. Chem. Chem. Phys. 18 (31) (2016) 21278–21287, https://doi.org/10.1039/c6cp01528j.

[27] Y.F. Kang, Y.H. Li, Y.W. Fang, Y. Xu, X.M. Wei, X.B. Yin, Carbon quantum dots for Zebrafish Fluorescence imaging, Sci. Rep. 5 (July) (2015), https://doi.org/10.1038/srep11835.

[28] D. Jiang, et al., Synthesis of luminescent graphene quantum dots with high quantum yield and their toxicity study, PLoS One 10 (12) (2015) pp, https://doi.org/10.1371/journal.pone.0144906.

[29] X. Ma, S. Li, V. Hessel, L. Lin, S. Meskers, F. Gallucci, Synthesis of luminescent carbon quantum dots by microplasma process, Chem. Eng. Process. - Process Intensif. 140 (January) (2019) 29–35, https://doi.org/10.1016/j.cep.2019.04.017.

[30] A.P. Savintsev, Y.O. Gavasheli, Z.K. Kalazhokov, K.K. Kalazhokov, X-ray photoelectron spectroscopy studies of the sodium chloride surface after laser exposure, J. Phys. Conf. Ser. 774 (1) (2016) pp, https://doi.org/10.1088/1742-6596/774/1/012118.

[31] Y. Wei, L. Chen, J. Wang, X. Liu, Y. Yang, S. Yu, Investigation on the chirality mechanism of chiral carbon quantum dots derived from tryptophan, RSC Adv. 9 (6) (2019) 3208–3214, https://doi.org/10.1039/c8ra09649j.

[32] S. Baskaya, M. Cesme, Synthesis of N-doped carbon quantum dots by hydrothermal synthesis method and investigation of optical properties, Turkish J. Nat. Sci. 10 (2) (Dec. 2021) 206–211, https://doi.org/10.46810/tdfd.956504.

[33] W. Wei, et al., Full-faradaic-active nitrogen species doping enables high-energy-density carbon-based supercapacitor, J. Energy Chem. 48 (Sep. 2020) 277–284, https://doi.org/10.1016/j.jechem.2020.02.011.

[34] R. Kumar, et al., An overview of recent progress in nanostructured carbon-based supercapacitor electrodes: From zero to bi-dimensional materials, Carbon 193. Pergamon (Jun. 2022) 298–338, https://doi.org/10.1016/j.carbon.2022.03.023.

[35] M. Athika, A. Prasath, E. Duraisamy, V. Sankar Devi, A. Selva Sharma, P. Elumalai, Carbon-quantum dots derived from denatured milk for efficient chromium-ion

sensing and supercapacitor applications, Mater. Lett. 241 (Apr. 2019) 156–159, https://doi.org/10.1016/j.matlet.2019.01.064.

[36] S. Sagar Mittal, G. Ramadas, N. Vasanthmurali, V.S. Madaneshwar, M. Sathish Kumar, N.K. Kothurkar, "Carbon quantum dot-polypyrrole nanocomposite for supercapacitor electrodes", *IOP Conf. Ser*, Mater. Sci. Eng. 577 (1) (Nov. 2019), 012194, https://doi.org/10.1088/1757-899X/577/1/012194.

[37] Q. Li, H. Cheng, X. Wu, C.F. Wang, G. Wu, S. Chen, Enriched carbon dots/graphene microfibers towards high-performance micro-supercapacitors, J. Mater. Chem. A 6 (29) (Jul. 2018) 14112–14119, https://doi.org/10.1039/c8ta02124d.